days before encounter). The spatial resolution would allow either instrument to separate the orbital and planetary emissions. In interpreting the Pioneer 10 UV observations, Carlson and Judge (*10*) assumed that all of the signal in the long-wavelength channel when Jupiter was in the field was due to hydrogen Ly α. Based on this assumption, the disk-averaged brightness was 400 R. The Voyager UV spectrometer measurement of hydrogen Ly α radiation was 14 kR averaged over the disk, a factor of 35 greater than the Pioneer 10 value. With the elongation point of Io's orbit in the field of view of the Pioneer 10 UV photometer, a signal in the long-wavelength channel was interpreted as 300 R of Ly α. No measurable emission was recorded in the short-wavelength channel (200 to 800 Å). The Voyager UV spectrometers recorded as much as 200 R in a single feature at 685 Å in the torus. This emission would have resulted in a prominent signal in both the UV photometer channels of Pioneer 10. We are satisfied that the Jupiter-Io system has undergone a major change since the Pioneer 10 encounter.

The results suggest that a high-temperature plasma torus was not present during the Pioneer 10 encounter in 1973 and that auroral activity was probably at a low level. These observations are consistent with a relationship between the presence of the plasma torus and auroral activity in the atmosphere of Jupiter, as suggested above.

Other evidence for major temporal changes in the Jupiter spectrum is found in the various measurements of hydrogen Ly α emission. The differences among these measurements appear to go beyond experimental uncertainties. Measurements from the Copernicus satellite (*14*) and earlier rocket measurements (*15*) range from 1.2 to 4 kR. More recent rocket measurements (*16*) (1 December 1978) produced a disk-averaged brightness of 13 kR. A measurement with the International Ultraviolet Explorer Instrument (*16*) on 9 December 1978 provided a subsolar brightness (averaged over 11 × 23 arc-seconds) of 12 to 14 kR, in substantial agreement with the Voyager UV spectrometer observations. Apparent variations in UV planetary albedo have also been recorded in earlier work (*17*).

It is clear that continuing Earth-based observations are necessary to aid our understanding the variability of the planetary system. Periodic observations of the Jupiter disk and polar auroral regions in H and H_2 emission are recommended, along with UV albedo measurements at longer wavelengths. The Io plasma torus is of special interest and attempts should be made to observe some of the emission characteristics of the higher-temperature components. The Voyager UV spectrometer data base on the torus will ultimately span a period of a least 2 years.

A. L. BROADFOOT
M. J. S. BELTON, P. Z. TAKACS
Kitt Peak National Observatory, Tucson, Arizona 85726
B. R. SANDEL, D. E. SHEMANSKY
Space Sciences Institute, University of Southern California Tucson Laboratories, Tucson, Arizona 85713
J. B. HOLBERG
Planetary Science Institute, Pasadena, California 91101
J. M. AJELLO
Jet Propulsion Laboratory, Pasadena, California 91103
S. K. ATREYA, T. M. DONAHUE
University of Michigan, Ann Arbor 48109
H. W. MOOS
Johns Hopkins University, Baltimore, Maryland 21218
J. L. BERTAUX, J. E. BLAMONT
Service d'Aeronomie du CNRS, Paris, France
D. F. STROBEL
Naval Research Laboratory, Washington, D.C. 20375
J. C. MCCONNELL
York University, Ontario, Canada M3J 1P3
A. DALGARNO
R. GOODY, M. B. MCELROY
Harvard University, Cambridge, Massachusetts 02138

References and Notes

1. A. L. Broadfoot *et al.*, *Space Sci. Rev.* **21**, 183 (1977).
2. R. A. Brown and Y. L. Yung, in *Jupiter*, T. Gehrels, Ed. (Univ. of Arizona Press, Tucson, 1976), p. 1102.
3. J. W. Warwick, J. B. Pearce, R. G. Peltzer, A. C. Riddle, *Science* **204**, 995 (1979).
4. G. L. Siscoe and C. K. Chen, *Icarus* **31**, 1 (1977).
5. B. A. Smith, L. A. Soderblom, T. V. Johnson, A. P. Ingersoll, S. A. Collins, E. M. Shoemaker, G. E. Hunt, H. Masursky, M. H. Carr, M. E. Davies, A. F. Cook II, J. Boyce, G. E. Danielson, T. Owen, C. Sagan, R. F. Beebe, J. Veverka, R. G. Strom, J. F. McCauley, D. Morrison, G. A. Briggs, V. E. Suomi, *Science* **204**, 951 (1979).
6. R. W. Carlson, J. C. Bhattacharya, B. A. Smith, T. V. Johnson, B. Hidayat, S. A. Smith, G. E. Taylor, B. O'Leary, R. T. Brinkmann, *ibid.* **182**, 53 (1973).
7. A. L. Broadfoot, S. S. Clapp, F. E. Stuart, *Space Sci. Instrum.* **3**, 209 (1977).
8. A. L. Broadfoot, S. Kumar, M. J. S. Belton, M. B. McElroy, *Science* **185**, 166 (1974).
9. Y. L. Yung and D. F. Strobel, in preparation.
10. R. W. Carlson and D. L. Judge, *J. Geophys. Res.* **79**, 3623 (1974).
11. A. Vidal-Madjar, *Solar Phys.* **40**, 69 (1975).
12. A. I. Stewart, D. E. Anderson, Jr., L. W. Esposito, C. A. Barth, *Science* **203**, 777 (1979).
13. M. H. Acuña and N. F. Ness, *J. Geophys. Res.* **81**, 2917 (1976).
14. S. K. Atreya, Y. L. Yung, T. M. Donahue, E. S. Barker, *Astrophys. J.* **218**, L83 (1977).
15. G. J. Rottman, H. W. Moos, C. S. Freer, *ibid.* **184**, L89 (1973).
16. J. T. Clarke, W. G. Fastie, P. D. Feldman, H. W. Moos, H. A. Weaver, C. B. Opal, *Eos*, in press.
17. R. C. Anderson, J. G. Pipes, A. L. Broadfoot, L. Wallace, *J. Atmos. Sci.* **26**, 874 (1969).
18. We acknowledge the untiring effort of Susan Hanson, our Assistant Experiment representative at JPL, who was responsible for most of the detailed sequencing of our experimental observations. We also acknowledge the efforts and operations of all Voyager Project personnel, who have made this mission a success. Kitt Peak National Observatory is operated by the Association of Universities for Research in Astronomy, Inc., under contract with the National Science Foundation. The research described in this report was carried out by the Jet Propulsion Laboratory, California Institute of Technology, under NASA contract NAS 7-100.

23 April 1979

Magnetic Field Studies at Jupiter by Voyager 1: Preliminary Results

Abstract. *Results obtained by the Goddard Space Flight Center magnetometers on Voyager 1 are described. These results concern the large-scale configuration of the Jovian bow shock and magnetopause, and the magnetic field in both the inner and outer magnetosphere. There is evidence that a magnetic tail extending away from the planet on the nightside is formed by the solar wind–Jovian field interaction. This is much like Earth's magnetosphere but is a new configuration for Jupiter's magnetosphere not previously considered from earlier Pioneer data. We report on the analysis and interpretation of magnetic field perturbations associated with intense electrical currents (approximately 5 × 10^6 amperes) flowing near or in the magnetic flux tube linking Jupiter with the satellite Io and induced by the relative motion between Io and the corotating Jovian magnetosphere. These currents may be an important source of heating the ionosphere and interior of Io through Joule dissipation.*

The Voyager magnetic field experiment consists of dual low field (LFM) and high field (HFM) triaxial fluxgate magnetometer sensors and associated electronics with extensive redundancy for high reliability as well as correction for the spacecraft's magnetic field (*1*). One LFM is located at the tip of a 13-m boom; the other is mounted 5.6 m inboard. The total weight of the sensors plus electronics, including the two HFM instruments, is 5.6 kg, and the power required is 2.2 W. During encounter, the LFM's automatically ranged through seven (of eight possible) scales for maximum sensitivity [± 8.8 nanoteslas (nT)

0036-8075/79/0601-0982$00.50/0

to ± 6400 nT, with quantization steps of 0.0044 nT to 3.12 nT]. The sensor equivalent root-mean-square (rms) noise is 0.006 nT (0.01 to 8.3 Hz). The dual magnetometer method and the estimation of zero offsets yield a preliminary accuracy of ± 0.2 nT ± 0.1 percent of full scale. The vector field was measured every 60 msec, and averages over 1.92 seconds, 48 seconds, and 16 minutes are used in this report.

The present results are based on preliminary experiment data records (EDR's), some of which are incomplete, and predicted supplementary EDR's which describe the predicted trajectory and orientation of the spacecraft. Voyager 1 executed several maneuvers during the encounter period which are not yet accurately described, and these data have been omitted in our analyses. The experiment operated flawlessly throughout the encounter, and no deleterious effects of the intense radiation environment and exposure have been noted in the data processed to date.

Bow shock, magnetopause, and magnetosphere. Voyager 1 crossed the bow shock of Jupiter for the first time at 1434 universal time (UT) on 28 February (day 59) 1979 at a Jovicentric distance of 85.7 R_J (R_J = radius of Jupiter). There was a total of five bow shock encounters inbound to periapsis as shown in Fig. 1, the final one on day 61 at 1308 UT. Also shown are magnetopause crossings, the first and last of which occurred at 1956 UT, day 60, and 0220 UT, day 62, respectively. Nine crossings were tentatively identified from the magnetic field data, with other less certain possibilities remaining.

Magnetic coplanarity was used to estimate the direction perpendicular to the bow shock surface. This yielded an average for the set of five: $<\delta> = -4° \pm 13°$ and $<\lambda> = 171° \pm 9°$, where δ and λ are, respectively, latitude and longitude referenced to solar equatorial plane ($\lambda \equiv 180°$ is sunward). The nine magnetopause candidates were analyzed by determining the plane of minimum variance (*2*) of the magnetic field variation applied to 1.92-second averages. An average of $<\delta> = 3° \pm 13°$ and $<\lambda> = 165° \pm 11°$ was obtained with a straight line segment representing $<\lambda> = 165°$ shown in Fig. 1. The "thickness" of the magnetopause transition zones ranged from 3 to 13 minutes, averaging 6.5 minutes.

Identifications of the outbound magnetopause and bow shock crossings are not complete at this date (29 March 1979) but Fig. 1 shows first and last magnetopause candidates (MP-A and MP-B), at 0033 UT on day 74 and at 0520 on day 75, respectively, and for the first and last bow shocks (BS-A and BS-B) at 0706 UT on day 77 and 1305 on day 81, respectively. The minimum variance analysis, as applied to MP-A data, yielded $\delta = 21°$ and $\lambda = 127°$. No other outbound magnetopause or bow shock crossing has been analyzed. More precise bow shock normals will be determined when plasma data are available.

A model was constructed of a nominal magnetopause surface represented by a hyperbola in the Jupiter orbital plane, with symmetry about the x-axis being as-

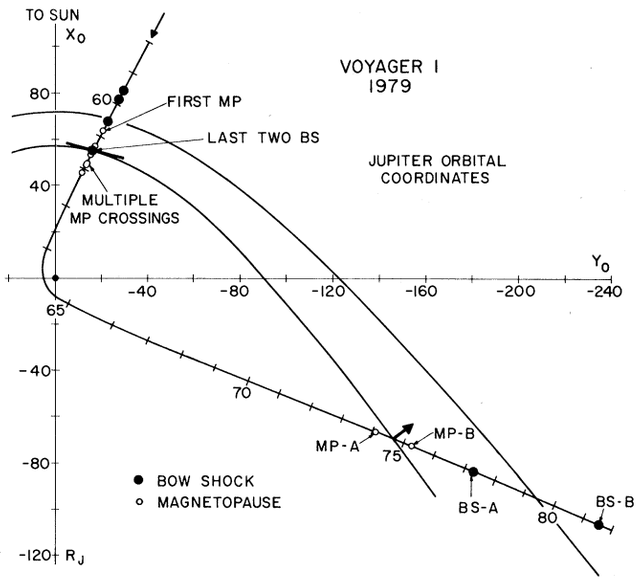

Fig. 1. Voyager 1 Jupiter encounter trajectory in Jupiter-centered orbital coordinates (x-y plane is the orbital plane, $+x$ toward the sun, $+z$ northward). The day of the year is labeled on the trajectory, which remains within 12.1 R_J of Jupiter's orbital plane over the interval shown.

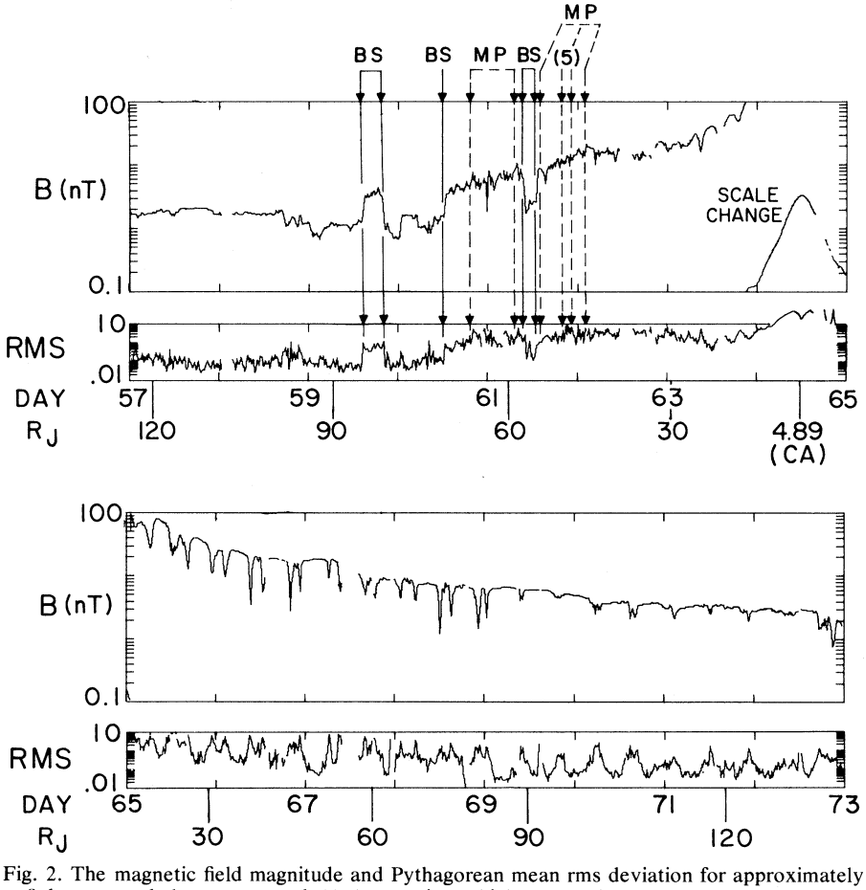

Fig. 2. The magnetic field magnitude and Pythagorean mean rms deviation for approximately ± 8 days around closest approach (*CA*) to Jupiter which occurred at 1205 UT on day 64, 1979. Inbound bow shock (*BS*) and magnetopause (*MP*) crossing times are denoted, as are a plot scale change.

Table 1. Preliminary Jovian dipole analyses. Model *IjEk* includes spherical harmonic terms up to order *j* for internal sources and *k* for external. Column 3 shows the number of data points at 4.8-minute intervals; column 4 shows magnitude in units Gauss-R_J^3; tilt (colatitude) and System III (1965) (longitude) are shown in degrees. The rms is Pythagorean mean of component rms values, and CN is the precondition number used in the matrix inversion.

Model	Radial extent (R_J)	Number	Magnitude	Colatitude	Longitude	rms	CN
I1E1	<9	119	3.98 ± 0.02	9.6° ± 0.2°	194° ± 2°	73	4
I2E1	<9	119	4.09	10.1°	189°	30	32
I1E1	<6	69	3.76	10.6°	189°	68	13
I2E1	<6	69	3.84 ± 0.04	13.3° ± 0.3°	190° ± 2°	11	
I3E0	<6		4.28	9.6°	202°	Model O_4	

sumed (see Fig. 1). The curve was constrained to intersect the inbound and outbound midpoints (that is, points midway between first and last crossings), and the slope inbound was made to agree with a $\lambda = 165°$ surface normal. Outbound the model predicts $\lambda = 126°$, which agrees very well with $\lambda = 127°$ observed. Similarly, a hyperbolic fit was made to the bow shock crossings, with the position of the focus and the *y*-axis scale factor being adjusted to force bow shock midpoint intersections. The average of the inbound bow shock normals was believed to be too uncertain to contribute good slope information. The predicted value of λ for the normal of the midpoint inbound bow shock set is $\lambda = 165°$, which agrees well with $< \lambda > = 171°$ given above. The model magnetopause and bow shock distances at the subsolar point give a ratio of 57/72 = 0.79 compared to Earth's, which is typically 0.69. The observed magnetopause crossings do not occur in the System III (1965) longitude interval predicted from Pioneer 10 and 11 data (*3*).

Figure 2 presents a summary of the magnetic field encounter data set, showing magnitude and mean component fluctuations (rms) observed during 16-minute averaging periods. A prominent feature is the recurrent decrease in the magnetic field intensity at approximately 5- or 10-hour intervals and always associated with increases in the rms. The steady increase of the rms near periapsis is due to spatial gradients of the magnetic field in the inner magnetosphere and not to intrinsic temporal fluctuations as seen elsewhere. The first peak in the rms after closest approach (CA) at ≈ 1500 UT is in part due to the Io flux tube currents. The dips in the field intensity correspond to passage of the spacecraft through a near equatorial current sheet, and usually occur in close proximity to the extended magnetic equatorial plane. In the inner magnetosphere, that is, at distances $< 12\ R_J$, the magnitude of the observed field was consistently below that predicted from the NASA-GSFC internal Jovian field model, O_4 (*4*), by several hundred nanoteslas. This suggests large-scale azimuthal currents in the Jovian magnetosphere.

The traditional method for the analysis and representation of planetary magnetic field data utilizes orthogonal spherical harmonic functions and assumes the magnetic field is derivable from a scalar potential. This is equivalent to assuming that there is no current flowing in the region of observations from which the unknown coefficients for the expansion are derived. Formal analyses of data taken within the inner magnetosphere of Jupiter are summarized in Table 1. The tilt and longitude of the dipole term are seen to be very close to the O_4 values. However, the magnitude of the moment obtained by these analyses is approximately 5 percent less than the O_4 values. We do not believe this represents a secular change of the planetary field but interpret it to be primarily due to the failure of the scalar potential mathemetical representation to be physically valid in the regions of space in which the observations were conducted. Future studies will address this issue.

Magnetodisc and magnetotail current sheets. Between 6 and 16 March (days 65 to 74) measurements were made in the nightside Jovian magnetosphere (see Figs. 1 and 2). During this period, intervals of perturbed field were observed during which |**B**| was reduced by ≥ 80 percent, the field had a southward component, and, through day 68, its azimuth (λ) changed. The character of these depressed field events is consistent with a diamagnetic plasma sheet and a thin embedded current sheet in which the direction of **B** changed.

Decreased fields in the plasma sheet were periodically observed out to the vicinity of the magnetopause, but the current sheet was not crossed beyond a distance of 80 R_J. During each 10-hour period out to 80 R_J, the spacecraft spent on average 3.2 ± 0.8 hours south of the current sheet and 6.8 ± 0.7 hours above it (the uncertainties are one standard deviation). Beyond 80 R_J, the depressions in |**B**| were seen at intervals of 10.0 ± 0.9 hours. Outside of the plasma sheet the observed field was extremely steady and oriented almost parallel to the heliographic equatorial plane ($\delta \sim 0°$) at an angle of $\lambda \sim 35°$ when the spacecraft was north of the current sheet and ~215° when south. These angles are consistent with the magnetic field approaching the direction parallel to the magnetopause at large distances (see Fig. 1, MP-A and MP-B), as well as with the earlier Pioneer 10 interpretation of a spiraling of the field (*5–8*).

Figure 3 shows the spacecraft locations during the perturbed field intervals in terms of both the longitude and radial distance. The south-to-north and north-to-south current sheet crossings are seen

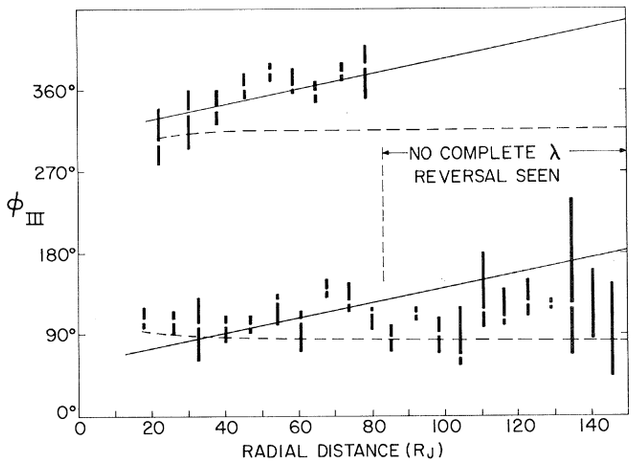

Fig. 3. The Jovicentric distance and extent in System III longitude of perturbed field regions. The gap in a bar marks the longitude at which the minimum field magnitude was observed. Out to a radial distance of about 80 R_J, the bars in the lower set represent south-to-north transitions; bars in the upper set represent the north-to-south crossings. Dashed curves indicate the longitudes at which the magnetic equator (rigid rotating disk) was crossed by the spacecraft (see text).

as the lower and upper sets, respectively. Both types of crossings were delayed in longitude (and time) relative to the prediction (*5*) for a rigid disk (dashed lines). The magnitude of the delay increases with distance from the planet. It is significant that the delay and its change with distance were more pronounced for the north-to-south crossings than for the south-to-north cases. That Voyager did not cross the current sheet beyond 80 R_J implies a warping of the sheet such that it did not reach the latitude of the spacecraft.

Several types of distortion of an equatorial disk-shaped current sheet can give an increasing delay (*5, 6*). On the basis of the Pioneer 10 observations (*7*), a spiral-shaped distortion has been considered by several investigators (*8*). Such a distortion implies a straight line on a System III (1965) longitude-R_J plot of the current sheet crossings. Figure 3 shows such lines drawn with the slope found (*8*) from a fit to the Pioneer 10 outbound current sheet crossings. The south-to-north Voyager 1 crossings are closer to the curve for an undistorted disk, whereas the north-to-south crossings are closer to the curve for a disk with spiral distortion. A distortion due to centrifugal forces also has been suggested (*7*), but this implies symmetry between the two types of crossings.

Another possible type of current sheet distortion, not considered in the literature for Jupiter, is a bending of the tailward part of the equatorial current sheet toward being parallel to the solar wind flow direction as an extended magnetotail like Earth's forms. For a spacecraft located above the Jovian equatorial plane, this distortion would appear maximum when the line of intersection between the magnetic equatorial plane and the Jovian equatorial plane has a dawn-dusk orientation and the northern half of the current disk is tailward. Voyager south-to-north crossings occurred near times when the sheet deformation was small and therefore were more consistent with the rigid disk model. The north-to-south crossings occurred when the bending of the tailward half of the current sheet away from the magnetic equatorial plane was large, and thus they occurred with a lag, relative to magnetic equatorial plane crossings, that increased with distance.

Further support for the concept of a transition to a magnetic tail configuration with increasing distance comes from examination of the structure of the observed current sheets. One can distinguish two classes of current sheets. One is characterized by a decrease in magnetic field intensity to a minimum significantly different from zero ($\geq$ several nanoteslas) and a rotation of field direction by $< 180°$, and the other by a decrease in magnetic field intensity to nearly zero ($\lesssim 1$ nT) and an $\approx 180°$ change (reversal) in magnetic field direction. Examples of the first class of current sheets are shown in Fig. 4a. A minimum variance analysis showed that the magnetic field direction in crossings A and C changed by means of a rotation of one component of **B** in a plane whose normal was $\delta = -75°$ in case A and $\delta = -86°$ in case C. Current sheets of this class were observed principally inbound and near Jupiter outbound.

Examples of the second class of current sheets are shown in Fig. 4b. They resemble the changes that are expected for a magnetic "tail," and indeed they were observed when Voyager 1 was tailward of and at larger distances from Jupiter. The difference between the two classes of crossings shown in Fig. 4 may thus represent a transition from corotating closed field lines near Jupiter ($\lesssim 25$ R_J) to more distended or open field lines farther from the planet as the magnetic tail region was penetrated by Voyager 1.

Io flux tube observations. A distinct magnetic field perturbation due to intense electrical currents induced by Io was observed when the spacecraft approached the minimum distance of 20,500 km south of the satellite at 1505 UT on 5 March. Passage through Io's flux tube, the ensemble of Jovian field lines penetrating the satellite, had been predicted to occur between 1502 and 1507 UT on the basis of the GSFC O_4 model. No noticeable change in field intensity was detected but there were significant directional changes.

To study the perturbation, we estimated the components of the local Jovian field individually by a regression analysis; we excluded the data most obviously affected by Io's presence. (The present analysis is still preliminary because of the lack of final attitude-orbit information.) After subtraction of the Jovian field, the perturbation field vectors, $\Delta\mathbf{B}$, lie approximately in a plane transverse to the background field. We define a right-handed orthogonal coordinate

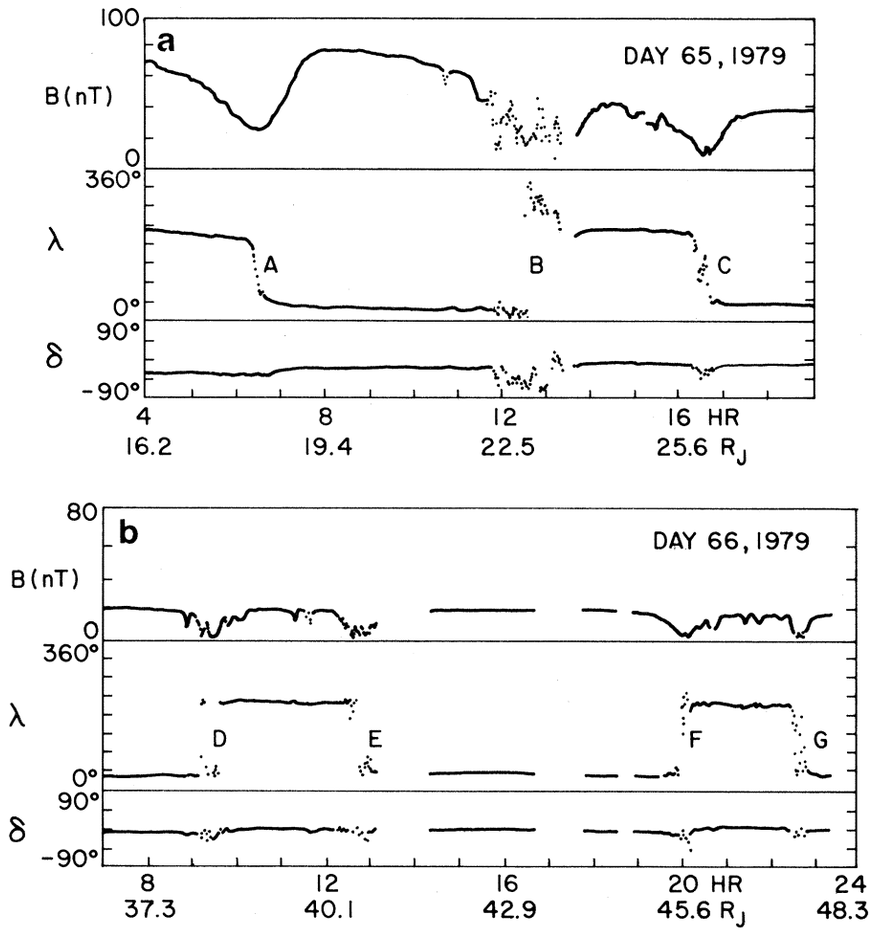

Fig. 4. Jovian field intensity dips or decrease events. (a) The class seen near Jupiter. (b) A second class which is observed at large distances outbound. The latter resemble "neutral" sheet crossings seen in Earth's magnetic tail. The angles are given in heliographic coordinates.

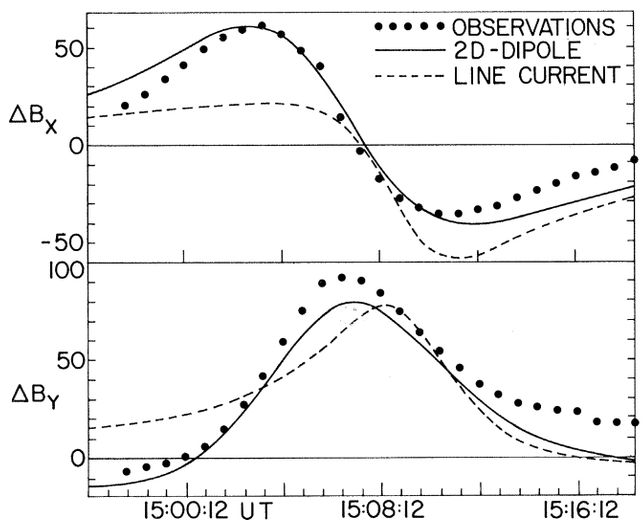

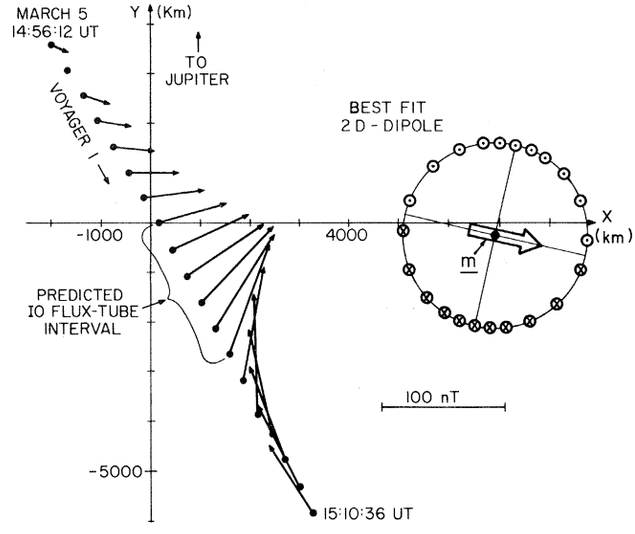

Fig. 5 (left). Comparison of observed perturbation magnetic field components ΔB_x, ΔB_y, and best-fit magnetic fields for twin oppositely directed currents and for a line current. The line current is located at $x_D = 5130$ km and $y_D = -3730$ km and has a strength of 1.1×10^6 A. The twin currents are located at $x_D = 6950$ km and $y_D = -200$ km with a strength 1.3×10^{10} A · km. Fig. 6 (right). Magnetic perturbation vector $\Delta\mathbf{B}$ in the x-y plane of coordinates used in our analyses (see text). The dipole source can be represented by a current of 4.8×10^6 A distributed over a cylindrical surface of one Io diameter with variable intensity according to a cosine law. The uncertainties of the regression analysis may be expressed as follows: $\mu_0|\mathbf{m}|/2\pi d^2_{\min} = 85 \pm 10$ nT, where $d_{\min}$ is the distance of the dipole from the trajectory in the x,y plane and $|\mathbf{m}|$ the dipole moment. In addition $|\mathbf{m}| = (1.2 \times 0.4) \times 10^{10}$ A · km and $y_D = -700 \pm 700$ km. The direction of the 2D-dipole moment is shown by the large arrow and is 15° outward from the direction of Io's velocity.

system centered at, and moving with, Io with the z-axis parallel to the background field and the x-axis located in the plane of the z-axis and the direction of corotational magnetospheric flow at Io. Inspection of the data at the highest possible time resolution shows that the field variation near Io is indeed very smooth and few, if any, fluctuations are observed at short time scales. The maximum perturbation is 94 nT at 1505 UT.

Figure 5 shows the components of the measured magnetic perturbation field together with least-mean-squares fits of a line current source antiparallel to the z-axis and a two-dimensional (2D) dipole source at locations $\mathbf{D} = (x_D, y_D)$ also determined by the best fit. The field of the 2D-dipole source is given by $\Delta\mathbf{B} = -\mu_0\nabla\Psi$ where

$$\Psi(\mathbf{x}) = \frac{\mathbf{m} \cdot (\mathbf{x} - \mathbf{D})}{2\pi|\mathbf{x} - \mathbf{D}|^2} \qquad (1)$$

with the position vector $\mathbf{x} = (x,y)$ and the 2D-magnetic moment $\mathbf{m} = (m_x, m_y)$ defined in the x,y-plane. We note that a 2D-dipole occurs as the lowest order term in the expansion of a system of currents parallel or antiparallel to the z-axis with zero net current. The symbol $\mathbf{m}$ can simply be considered as the magnetic moment per unit length in the z-direction. For two opposite line currents the value $|\mathbf{m}|$ is given by current times distance. Figure 6 shows the trajectory projected on the x,y-plane together with the vectors $\Delta\mathbf{B}$ and the best-fit 2D-dipole. This analysis shows that the 2D-dipole fit is quite reasonable and is much better than the line current fit. It should be noted that the small linear extent of the magnetic field anomaly, full width–half maximum = 9,000 km, when compared to the distance to Io, 20,500 km, and the lack of intensity perturbations, effectively rule out an intrinsic field of Io as the source of the observed anomaly.

The smooth variation of $\Delta\mathbf{B}$ and the good fit to a 2D-dipole are in agreement with the idea that Voyager passed very close to a current system with upward and downward currents of about equal magnitude along the z-axis but did not actually penetrate the region of maximum current flow. This observational result is in agreement with the physical concept of Io's role as a unipolar generator proposed 10 years ago (*9*) and later extended (*10*). The electric field is set up in Io because of its motion relative to the corotating magnetospheric plasma, and this drives a current system through the conducting path formed by Io, Io's ionosphere, field-aligned currents in the Jovian magnetosphere, and transverse currents through the Jovian ionosphere. In a more accurate description the field-aligned currents are replaced by a current system of standing Alfvén waves, which also involve nonfield-aligned current components (*11*). A more refined physical modeling of the observations is deferred to a later study.

The large currents may be the source for offset of the location of the Io flux tube footprint near Jupiter, which can explain the asymmetry of the observed Io-modulated decametric emission pattern (*9, 13*). Note that the 2D-dipole is offset by 7,000 km out of 20,500 km or an equivalent angle of 19°. This offset is, of course, the reason for the failure of Voyager 1 to penetrate the flux tube as planned.

The power dissipation implied in the current loop set up by Io's interaction with the Jovian magnetosphere leads to a Joule heating of $P \approx 10^{12}$ W. This value is rather model independent and is given by $P = m_x \cdot E_{\text{Io}}$ where $E_{\text{Io}} = v_{\text{rel}} \cdot B_{\text{Io}}$ with $v_{\text{rel}} = 57$ km/sec and $B_{\text{Io}} \approx 1900$ nT. The value of P is close to the value obtained from tidal dissipation (*12*). Since electrical currents flow in paths of least resistance, internal hot springs in Io might develop where the current cross section narrows in the interior of Io. As the temperature rises, so does the conductivity, and this may lead to an intensification or runaway of energy dissipation in the form of Joule heating. We point to the possible role of this Joule heating for Io and the Io plasma torus.

NORMAN F. NESS
MARIO H. ACUÑA
RONALD P. LEPPING
LEONARD F. BURLAGA
KENNETH W. BEHANNON
Goddard Space Flight Center, Greenbelt, Maryland 20771
FRITZ M. NEUBAUER
Technische Universität, Braunschweig, Federal Republic of Germany

References and Notes

1. K. W. Behannon, M. H. Acuña, L. F. Burlaga, R. P. Lepping, N. F. Ness, F. M. Neubauer, *Space Sci. Rev.* **21**, 235 (1977).
2. B. U. O. Sonnerup and L. J. Cahill, *J. Geophys. Res.* **72**, 171 (1967).
3. A. J. Dessler and V. M. Vasyliunas, *Geophys. Res. Lett.* **6**, 37 (1979).
4. M. H. Acuña and N. F. Ness, *J. Geophys. Res.* **81**, 2917 (1976).
5. J. A. Gledhill, *Nature (London)* **214**, 156 (1967); C. K. Goertz, *J. Geophys. Res.* **81**, 3368 (1976).
6. L. J. Gleeson and W. I. Axford, *J. Geophys. Res.* **81**, 3403 (1976).
7. E. J. Smith, L. Davis, Jr., D. E. Jones, P. J. Coleman, Jr., D. S. Colburn, P. Dyal, C. P. Sonett, A. M. A. Frandsen, *ibid.* **79**, 3501 (1974).
8. T. G. Northrop, C. K. Goertz, M. F. Thomsen, *ibid.*, p. 3579; D. E. Jones, E. J. Smith, L. Davis, Jr., D. S. Colburn, P. J. Coleman, Jr., P. Dyal, C. P. Sonett, *Utah Acad. Sci. Arts Lett. Proc.* **51**, 153 (1974); A. Eviatar and A. I. Ershkovich, *J. Geophys. Res.* **81**, 4027 (1976); M. G. Kivelson, P. J. Coleman, Jr., L. Froidevaux, R. L. Rosenberg, *ibid.* **83**, 4823 (1978).
9. J. H. Piddington and J. F. Drake, *Nature (London)* **217**, 935 (1968); P. Goldreich and D. Lynden-Bell, *Astrophys. J.* **156**, 59 (1969).
10. S. D. Shawhan, C. K. Goertz, R. F. Hubbard, D. A. Gurnett, G. Joyce, in *The Magnetospheres of the Earth and Jupiter*, V. Formisano, Ed. (Reidel, Dordrecht, 1975); J. H. Piddington, *Moon* **17**, 373 (1977).
11. S. D. Drell, H. M. Foley, M. A. Ruderman, *J. Geophys. Res.* **70**, 3131 (1965).
12. S. Peale, P. Cassen, R. T. Reynolds, *Science* **203**, 892 (1979).
13. See, for example, R. A. Smith, in *Jupiter*, T. Gehrels, Ed. (Univ. of Arizona Press, Tucson, 1976), figure 2 and pp. 1146–1189.

14. We thank our colleagues in the Voyager project for discussions of these early results and the entire Voyager project team for the success of this experiment. We also thank G. Sisk, E. Franzgrote, and J. Tupman of the JPL for their support; C. Moyer, J. Scheifele, J. Seek, and E. Worley for contributions to the design, development, and testing at GSFC of the experiment instrumentation; and T. Carleton, P. Harrison, D. Howell, W. Mish, L. Moriarty, A. Silver, and M. Silverstein of the data analysis team for contributing to the success of the rapid magnetic fields and plasma particles data processing system. F.M.N. was supported financially by the German Ministry of Science and Technology.

20 April 1979

Plasma Observations Near Jupiter: Initial Results from Voyager 1

Abstract. *Extensive measurements of low-energy positive ions and electrons were made throughout the Jupiter encounter of Voyager 1. The bow shock and magnetopause were crossed several times at distances consistent with variations in the upstream solar wind pressure measured on Voyager 2. During the inbound pass, the number density increased by six orders of magnitude between the innermost magnetopause crossing at ~ 47 Jupiter radii and near closest approach at ~ 5 Jupiter radii; the plasma flow during this period was predominately in the direction of corotation. Marked increases in number density were observed twice per planetary rotation, near the magnetic equator. Jupiterward of the Io plasma torus, a cold, corotating plasma was observed and the energy/charge spectra show well-resolved, heavy-ion peaks at mass-to-charge ratios* A/Z* = *8, 16, 32, and 64.*

The Voyager plasma experiment is a cooperative effort by experimenters from the Massachusetts Institute of Technology, the Goddard Space Flight Center, the Jet Propulsion Laboratory, the High Altitude Observatory of the National Center for Atmospheric Research, the University of California at Los Angeles, and the Max-Planck-Institut für Aeronomie. The instrument and the experimental objectives have been described in detail (*1*) and only a brief summary is given here. The instrument consists of four Faraday cup sensors. Three of these (the A, B, and C cups) are arranged in a symmetric cluster whose axis usually points toward Earth. The axis of the fourth sensor (the D cup) is at right angles to the axis of the cluster and points roughly into the direction of corotational flow on the inbound leg of the trajectory at Jupiter; see Fig. 1. The energy range for protons and electrons is 10 to 5950 eV. The L and M modes are positive ion modes spanning this energy/charge range in 16 contiguous steps (29 percent nominal resolution in energy) and 128 contiguous steps (3.6 percent nominal resolution in energy), respectively. Positive ion measurements are made with all four sensors. Electron measurements are made only with the D sensor. The E1 mode measures electrons with energies in the range 10 to 140 eV, using 16 contiguous steps at 3.6 percent nominal resolution in energy. The E2 mode measures electrons with energies in the range 10 to 5950 eV, using 16 contiguous steps at 29 percent nominal resolution in energy. During encounter, the time required for a complete measurement cycle of four modes is 96 seconds.

In this report we describe (i) the observed crossings of the bow shock and magnetopause and the changes in their positions with external conditions, (ii) plasma properties in the dayside outer magnetosphere, (iii) properties of the plasma in the inner magnetosphere, (iv) plasma properties in the nightside outer magnetosphere, and (v) radiation effects on the performance of the instrument. The reader should bear in mind that results given here are based on a very preliminary state of the analysis. For example, the positive ion densities quoted for the inbound pass for the outer magnetosphere are based on assumptions that are only partially true, such as that the flow is corotational and supersonic and that all of the ions are protons. The first two assumptions will have to be modified and the third is certainly wrong. For this reason, no precise estimate can be given of the accuracy of the densities shown in Fig. 3. They are probably good to a factor of 5, but a final determination can only be made on the basis of a more detailed analysis. Densities quoted for the inner magnetosphere are much more accurate, for reasons which will become apparent below.

Bow shock and magnetopause crossings seen by Voyager 1 on the inbound and outbound trajectories are listed in Table 1 and shown on the trajectory plot in Fig. 1. Figure 2 shows the upstream pressure measured by Voyager 2 and extrapolated to Voyager 1, taking into account corotation delay and the different radial distances of the two spacecraft from the sun. The latter effect was the major source of delay; a typical delay time between observation at Voyager 2 and arrival at Voyager 1 was ~ 35 hours. The first bow shock crossing occurred at 85.5 Jupiter radii (R_J) at a dynamic pressure of 8×10^{-10} dyne/cm^2. Using these values of pressure and distance, P_0 and R_0, the five shock crossings observed on the inbound pass fit extremely well the relationship $P = P_0(R_0/R)^\delta$ with $\delta = 3$. This characterization agrees with that of Smith *et al.* (*2*) and confirms the conclusion of the Pioneer experimenters that Jupiter's magnetosphere is much more compressible than that of Earth. The dashed curve of Fig. 2 represents the equilibrium position of the bow shock versus pressure given by the relation above; similarly, the solid curve shows the expected position of the magnetopause, using $\delta = 3$ and a value of R_0 appropriate for the initial position of the magnetopause rather than the bow shock. The agreement with actual crossings is good.

The six magnetopause crossings observed on the inbound and outbound passes occurred at subspacecraft System III (1965) longitudes ranging from 10° to 173°; the prediction by Dessler and Vasyliunas (*3*) of a tendency for magnetopause crossings to cluster in the range 290° ± 65°, based on the presence of such a tendency in the Pioneer 10 and 11 observations, was not confirmed.

In the dayside outer magnetosphere, plasma ions exhibit a strong corotational signature on the inbound pass, as evidenced by a consistently enhanced signal in the D cup as compared to ion currents

0036-8075/79/0601-0987$00.50/0